

CONVECTIVE SYSTEM STRUCTURE OVER SOUTHEASTERN SOUTH AMERICA FROM TRMM OBSERVATIONS

Paola Salio ⁽¹⁾, Luciano Vidal ⁽¹⁾, Edward Zipser ⁽²⁾ and Chuntao Liu ⁽²⁾

⁽¹⁾ Departamento de Ciencias de la Atmósfera y los Océanos. UBA.
Centro de Investigaciones del Mar y la Atmósfera. CONICET – UBA.
Buenos Aires. Argentina.

⁽²⁾ Department of Meteorology. University of Utah. Salt Lake City. Utah. USA

1. INTRODUCTION

Global and regional characteristics of deep convection over South America have been analyzed by many authors based on different observing tools. Satellite infrared images have been the primary tool since the GOES constellation satellite was launched over the region. These data make it possible to understand the evolution and behavior of convective systems over many regions, especially over large areas without ground-based observations. Based on geostationary satellite information, Machado et al (1998), Velasco and Frisch (1987), among others showed the characteristics and structure of mesoscale convective systems over South America. However, there is an important lack of knowledge of the internal structure of convective systems over the area due to the sparse ground-based radar network.

The Tropical Rainfall Measuring Mission (TRMM) constellation (Kummerow et al., 1998) measures visible and infrared radiances (VIRS), microwave radiance from TRMM Microwave Imager (TMI), radar reflectivity from the Precipitation Radar (PR), and flashes from Lightning Imager Sensor (LIS). This unique dataset provides the opportunity to investigate the internal structure of convection mainly over tropical and subtropical areas and to describe the evolution of its diurnal cycle.

A prime motivation of this study is to generate a climatology and characterize the internal structure of the convection over Southeastern South America (SESA). This paper also describes the diurnal cycle of convection over SESA and the relationship between the internal structure of convection and different synoptic situations dominated by low level jets (LLJs).

2. METHODOLOGY

The University of Utah Version-6 TRMM level 3 dataset spatially and temporal collocate all available sensor information from TRMM constellation during a 9-year period (1998-2006, Liu et al., 2007). Radar Precipitation Features (RPFs) are defined as “a pure precipitation feature” because considering all Precipitation Features (Nesbitt et al., 2003) in the sample, with TRMM 2A25 surface rain rate greater than 0 mm h^{-1} . The characteristics of each feature are summarized from measurements and retrievals from PR, TMI, VIRS and LIS at grouped pixels. Parameters considered in this paper are as follows:

- Stratiform and convective rain area and volume, maximum height of 15, 20 and 40 dBz from algorithm 2A25
- 85 GHz Polarized Corrected Temperature (PCT) from TMI,.
- minimum temperature brightness temperature (T_{B11}) from IR image.
- Number of lightning flashes from LIS.

Corresponding Author Address: Dr. Paola Salio. salio@cima.fcen.uba.ar
Departamento de Ciencias de la Atmósfera y los Océanos. UBA. Bs. As. Argentina.

Synoptic situations associated with LLJ events are detected using GDAS, considering a criterion similar to

Bonner's(1968) already used in Salio et al (2002) and Nicolini et al (2004). Figure 1 shows the low level circulation for each studied event. Situations called Chaco Jet event (CJE) and No Chaco Jet event (NCJE) are known as South American Low Level Jet events (SALLJ), this being a particular categorization aimed at understanding the differences between tropical and subtropical latitudes. Cases associated with an anticyclonic circulation over Argentina are called Low Level Jet Argentina (LLJA) and situation without the presence of a LLJ over the area are called NoLLJ.

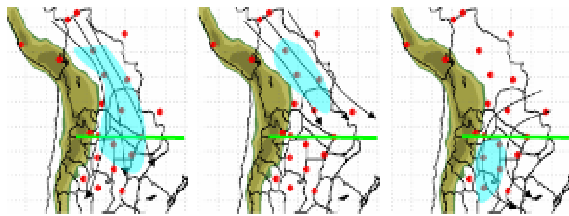


Figure 1: Scheme of the circulation of the wind in low levels under three characteristic low level jet events over Southeast South America. Chaco Jet Event is outlined at the top, on the center No Chaco Jet Event and at the bottom the Low Level Jet Argentina scheme. The area shaded in light blue display the isotach of 12ms^{-1} . The green line indicates the latitude of 25°S .

3. RESULTS

3.1 CONTINENTAL DESCRIPTION

The main dynamic systems that generate precipitation can be identified by the distribution of the RPFs during the four seasons of the year (Figure 2). These include the annual evolution of the Intertropical Convergence Zone, the South Atlantic Convergence Zone during summer, as well as the annual cycle of precipitation over the Altiplano with a maximum in summer and a minimum in winter. It is important to emphasize the maximum south of 30°S , as important as those over the Amazon region, displaying maximum frequency values in summer and spring. Figure 3 shows the frequency of RPFs with T_{B11} values lower than 210 K. This figure shows that the extreme events also tend to

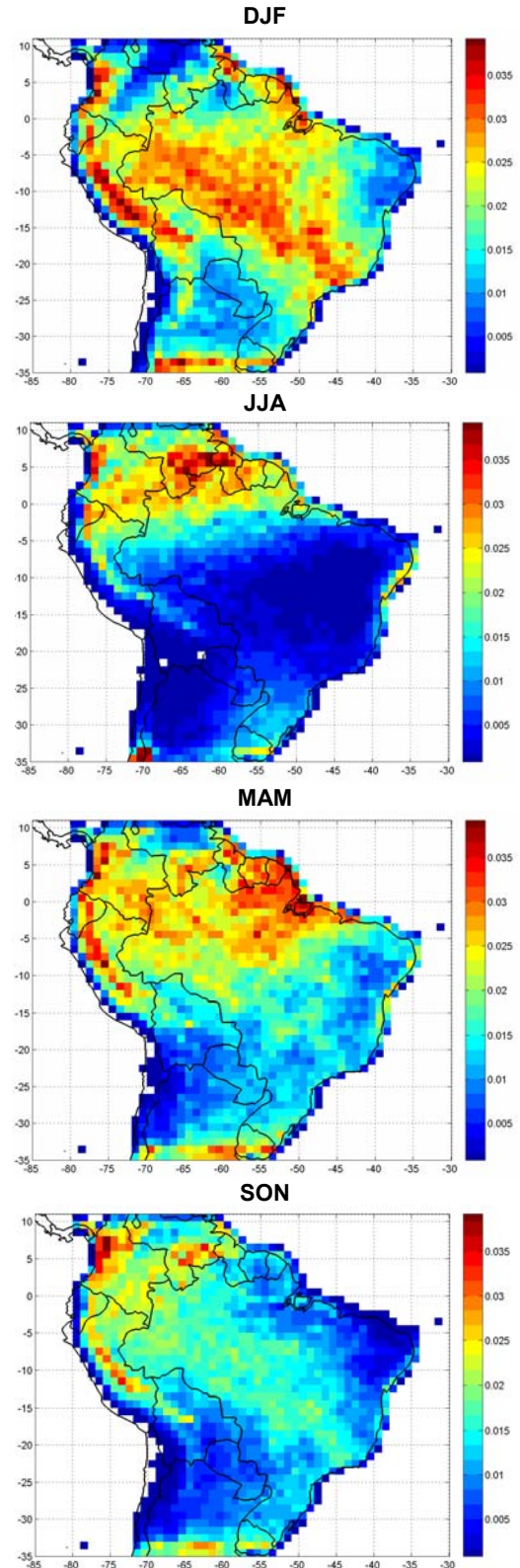


Figure 2: Number of RPFs per km^2 summarized onto a 1×1 degree resolution.

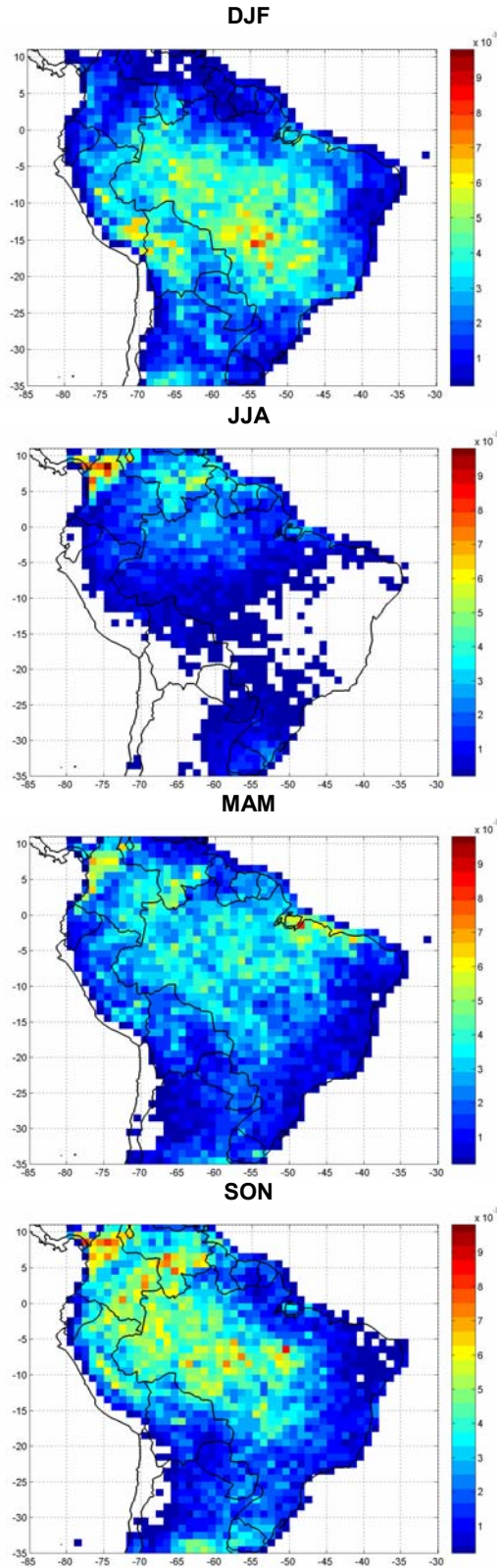


Figure 3: Number of RPFs per km² summarized onto a 1x1 degree resolution with T_{B11} lower than 210 K.

be located on the Amazon and SESA regions mainly during summer and spring. Extreme values of 20 dBz heights greater than 5 km indicate the presence of deep convection on the center of Argentina, Uruguay and the Altiplano especially during summer and spring (figure not shown).

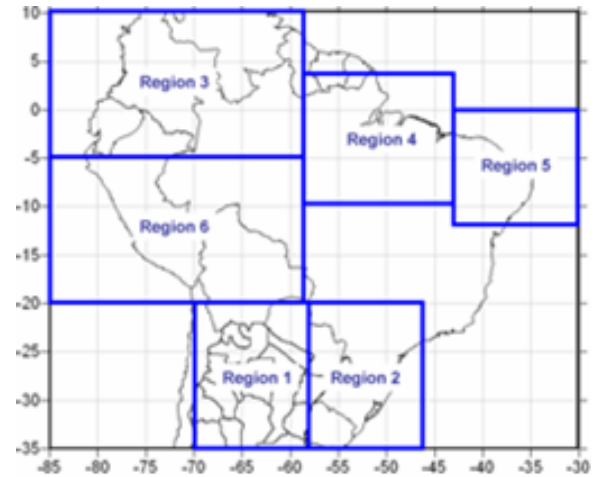


Figure 4: South American area and selected regions mentioned in the text.

Vertical profiles of the relative frequency of the maximum height of the 20 and 40 dBz contours measured from the radar over different selected regions are shown in figure 5. All regions have been indicated in figure 4. One significant finding is that fully 20% of RPFs contain a 40 dBZ radar reflectivity contour attaining an altitude greater than 10 km over SESA, reaching an extreme of 18 km over region 1, while in tropical areas 40 dBZ values are lower than 8 km altitude. Regions 3 to 6, characterized by a tropical behavior, show an important 40 dBZ frequency extreme at 4 km, while the maximum over SESA has the same mean altitude though lower intensity. This fact shows that the convection altitude tends to be higher in the subtropical area than in the tropical, where no cases are detectable up to 10 km. Zipser et al (2006) , Salio et al (2007), among others found that strong deep convective systems tend to occur over SESA during SALLJ situations, extreme results over subtropical area agree with those findings.

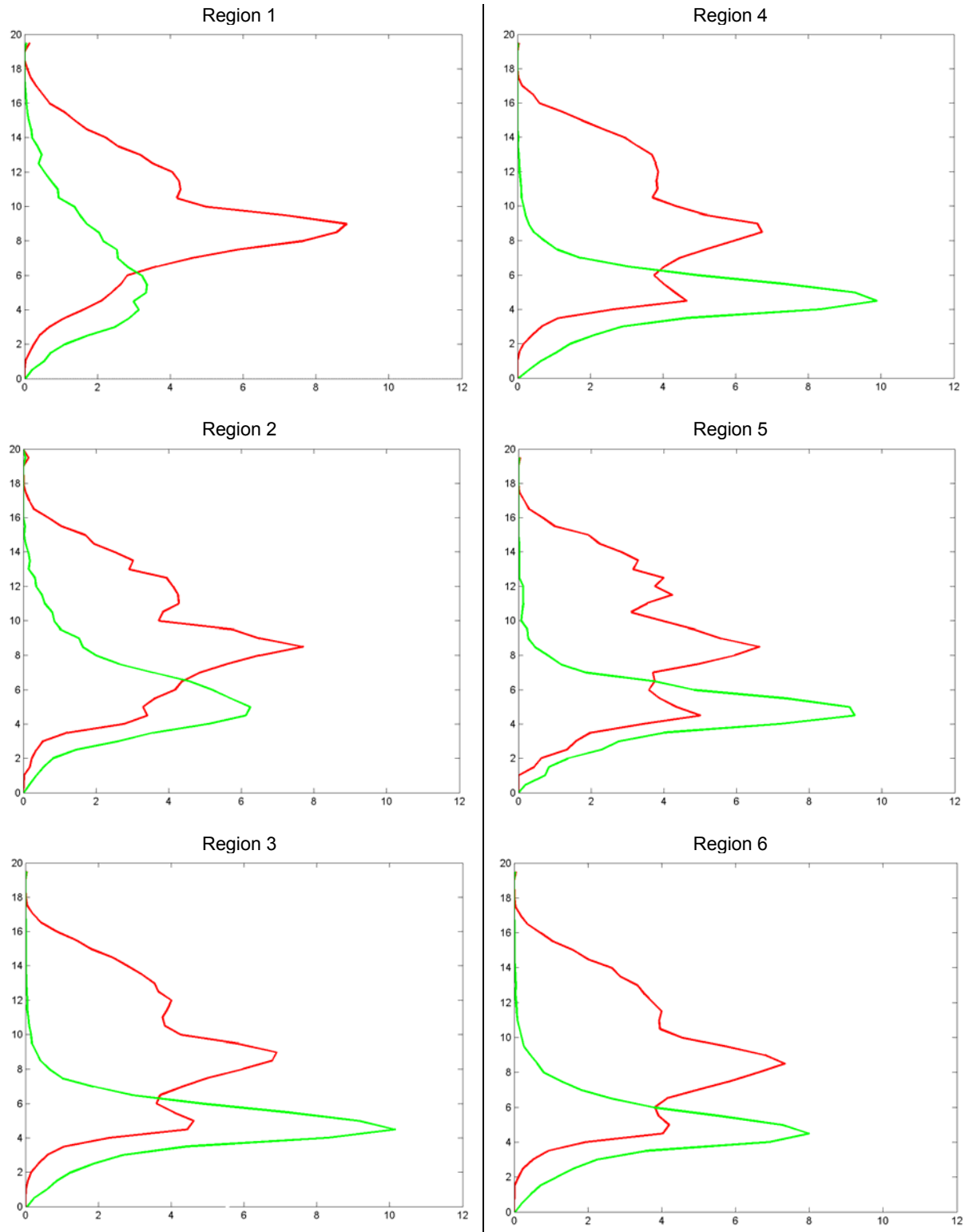


Figure 5: Relative frequency of maximum height of 20 (red line) and 40 (green line) dBZ for all RPFs in the sample, considering all seasons over the different regions showed in Figure 4.

Table 1 shows a number of parameters associated with extreme events. Parameters similar to those in Liuct et al (2007, Table 1 in their paper) have been calculated to compare the behavior of extreme RPF events over SESA. The frequency of occurrence of radar echo tops reaching 15 km shown in that table are 10-

times higher than the frequencies in the whole TRMM covered area, where only the 1% of the sample reaches this altitude (Liuct et al 2007). A similar behavior can be depicted from the frequency of PCT lower than 200 K, where values in the studied sample are much higher than in the whole sample.

#	Parameter	West	East
I	$T_{B11} \leq 210 \text{ K} (\%)$	11.4	9.2
II	$\text{MaxH } 40 \geq 10\text{km} (\%)$	14.1	8.5
III	$\text{MaxH } 20 \geq 15\text{km} (\%)$	10.3	8.8
IV	$\text{MaxH } 20 \geq 10\text{km} (\%)$	58.2	57.7
V	$\text{MIN85PCT} \leq 200\text{K} (\%)$	37.6	43.9
VI	$\text{MIN85PCT} \leq 225\text{K} (\%)$	47.8	54.2
VII	% Convective Area	27.24	19.9
VIII	Mean Volumetric Rain	21312.5	19901

Table 1: I) Percentage of RPFs with T_{B11} lower than 210 K. Considering only RPFs with T_{B11} lower than 210 K; II) Percentage of cases with maximum height of 40 dBz higher than 10 km; III) idem II for maximum height of 20 dBz higher than 15 km; IV) idem III for 10 km; V) idem II minimum PCT lower than 200 K; VI) idem V for 225 K; VII) Percentage of convective area of RPF from 2A25 algorithm and VIII) Mean Volumetric rain for all RPFs from 2A25 algorithm.

Some differences between western and eastern area of SESA need to be remarked. While region 1 (western area) tends to show a frequency of RPFs with lower T_{B11} and higher tops, PCT tends to be cooler over region 2 (eastern area). These findings are correlated with the presence of a greater convective area over region 1 and stronger volumetric rain rate.

An extended analysis of the seasonal cycle of extreme values over Region 1 and 2 is summarized in the next section.

3.2 SOUTHEASTERN SOUTH AMERICA CHARACTERISTICS UNDER DIFFERENT LLJ SITUATIONS

The analysis of the vertical profiles of the relative eco top height frequency of different dBz contours (15, 20 and 40) in region 1 and 2 reveals that convective systems are deeper during DJF and SON

in the western region, though in a lower degree. The most frequent height ranges from 3 to 5 km for 40 dBZ in both regions. In the case of 15 and 20 dBz, the most frequent height in region 1 is between 5 and 7 km in the DJF period, 4 km in MAM and JJA and 5 km in SON. The eastern region displays values of 5 km in DJF, 4.5 km in MAM, and 4 km in JJA and SON. On the other hand, the 40dBZ curve reaches the ground during MAM and JJA in region 1, though more frequently in fall, which indicates some probability of precipitation on surface (figure not shown).

The relative frequency of top heights of the 15, 20 and 40 dBZ contours of CJE and LLJA cases in region 1 and 2 are shown in figures 6 and 7 respectively. Only the figures of the samples showing significant characteristics are presented. The most interesting feature is the system height during CJE events, mainly in DJF,

which reaches values above 8 km in more than 50% of the cases in the western region. In the east, systems are weaker and the nucleus of the maximum 40 dBz height is located at a greater altitude. The 40 dBz contour reaches the surface in both regions, which indicates the possibility of precipitation occurrence. The structure of the NCJEs is quite similar to the CJE cases

in both regions, confirming that there is an effect of SALLJ events altogether over SESA (figure not shown). Since maximum frequencies for the 40 dBz contour are located at 3 km and the contours are relatively weak during extreme events, LLJAs tend to be shallower in the seasons shown (DJF and SON) than the systems of CJE events (Figure 7).

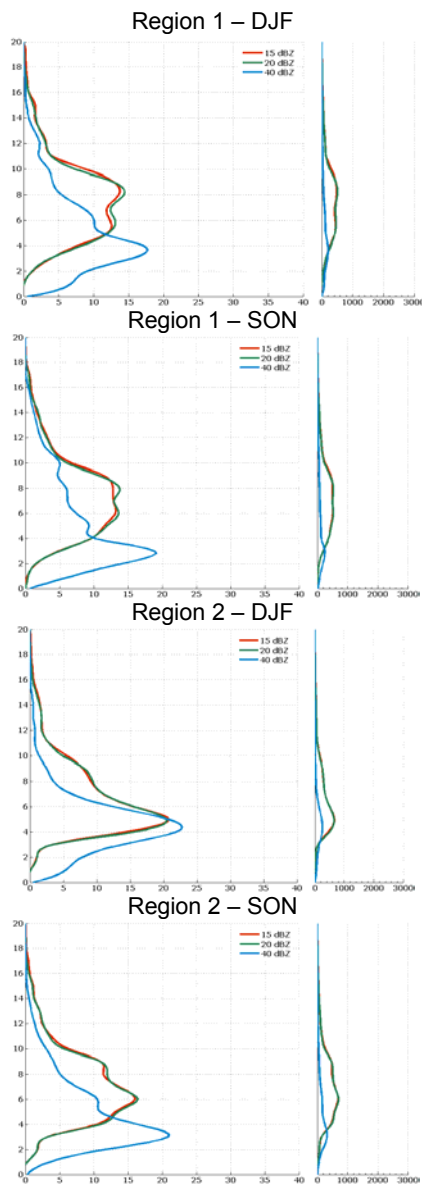


Figure 6: Relative frequency of maximum height of 15 (red), 20 (green) and 40 (blue) dBZ for all RPFs in the sample, considering the regions 1 and 2 showed in Figure 5 for two seasons and CJE situations. Each panel shows the number of RPFs at every level.

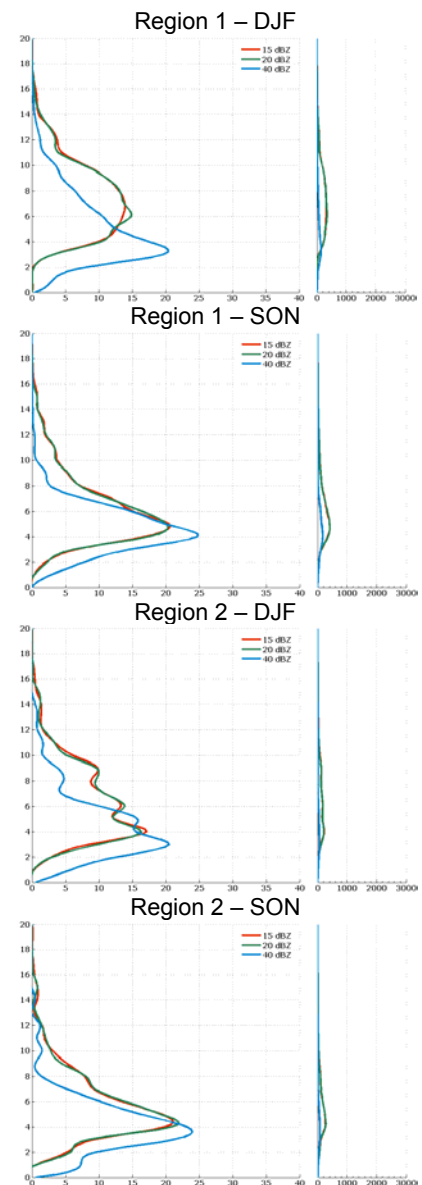


Figure 7: Relative frequency of maximum height of 15 (red), 20 (green) and 40 (blue) dBZ for all RPFs in the sample, considering the regions 1 and 2 showed in Figure 5 for two seasons and LLJA situations. Each panel shows the number of RPFs at every level.

3.3 DIURNAL CYCLE UNDER DIFFERENT LLJ SITUATIONS

In order to study the behavior of extreme convection under different LLJ situations, the diurnal cycle of the frequency of RPFs with volumetric rain higher than 5000 mm is shown in figure 9. The diurnal cycle of the SALLJ-related (CJE and NCJE) RPFs shows a nocturnal peak (06 UTC, 03 LT) in spring in western SESA, whereas the RPFs in eastern SESA have a maximum in phase with radiative heating. An afternoon maximum is extreme during NCJE in summer; on the contrary, a night-time maximum occurs during CJE suggesting a crucial role of the low level jet in CJE events and the radiative heating in NCJE. Previous studies suggest that the SALLJ brings high moisture and instability over SESA (Salio et al., 2007). The figure confirms this evidence given that strong convection over both areas does not occur in other SALLJ-related situations.

ACKNOWLEDGMENTS

This research was supported by UBA grant X266, ANPCyT grant N° PICT 07 – 14420, PIP 5582.

REFERENCES

Bonner, W. D., 1968: Climatology of the low level jet. *Mon. Wea. Rev.*, **96**, 833-850.

Kummerow, C., W. Barnes, T. Kozu, J. Shiue, and J. Simpson, 1998: The Tropical Rainfall Measuring Mission (TRMM) Sensor Package. *J. Atmos. Oceanic Technol.*, **15**, 809-817.

Liu, C., E. Zipser, and S. W. Nesbitt, 2007: Global distribution of tropical deep convection: Different perspectives using infrared and radar as the primary data source, *J. Climate*, **20**, 489-503.

Liu, C., E. J. Zipser, D. J. Cecil, S. W. Nesbitt, and S. Sherwood, 2008: A cloud and precipitation feature database from 9

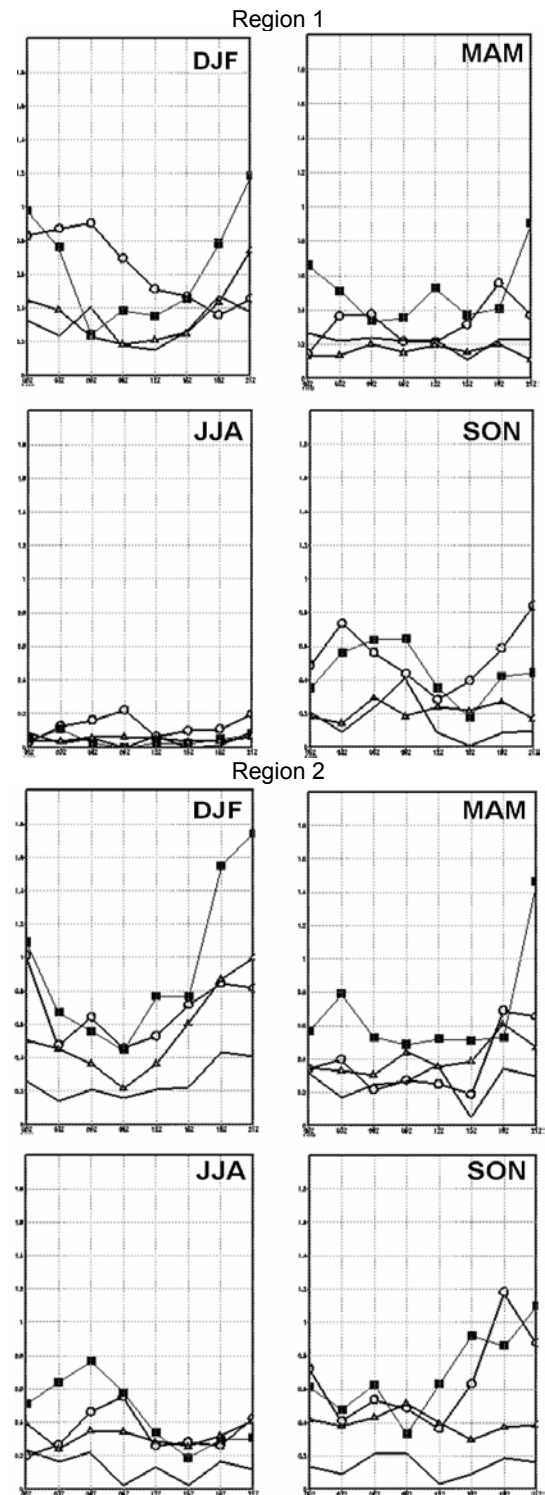


Figure 8: Diurnal cycle of frequency of RPFs with volumetric rain higher than 5000 mm during CJE (open circle), NCJE (bow filled), LLJA (none mark) and NoLLJ (open triangle). All season are presented in each panel.

years of TRMM observations. Submitted to *J. Appl. Meteor.*

Machado, L. A. T., W. B. Rossow, R. L. Guedes, and A. W. Walker, 1998: Life cycle variations of mesoscale convective systems over the Americas. *Mon. Wea. Rev.*, **126**, 1630-1654.

Nesbitt, S. W., and E. J. Zipser, 2003: The diurnal cycle of rainfall and convective intensity according to three years of TRMM measurements. *J. Climate.*, **16**, 1456–1475.

Nicolini, M., P. Salio, G. Ulke, J. Marengo, M. Douglas, J. Paegle, and E. Zipser, 2004: South American low level jet diurnal cycle and three dimensional structure. *CLIVAR Exchanges*, No. 9, International CLIVAR Project Office, Southampton, United Kingdom, 6-8.

Salio, P., M. Nicolini, and A. C. Saulo, 2002: Chaco low level jet events characterization during the austral summer season by ERA reanalysis. *J. Geophys. Res.*, **107**, 4816.

Salio, P., M. Nicolini, and E. J. Zipser, 2007: Mesoscale Convective Systems Over Southeastern South America and Their Relationship with the South American Low-Level Jet. *Mon. Wea. Rev.*, **135**, 1290-1309.

Zipser, E. J., D. Cecil, C. Liu, S. Nesbitt, and D. Yorty, 2006: Where are the most intense thunder storms on earth?, *Bull. Amer. Meteor. Soc.*, **87**, 1057-1071.

Velasco, I. Y., and J. M. Fritsch, 1987: Mesoscale convective complexes in the Americas. *J. Geophys. Res.*, **92**, 9591-9613.